Overall controlling factor in R_1-R_2-D reactions-diffusion phenomena in two-reactions-in-series systems for selectivity enhancement

Musa Najimu[1,2,4*], Lateef Adewale Kareem[2,3], Sagir Adamu[2], Kandis Leslie Gilliard-AbdulAziz[4,5]

[1]Department of Chemical and Biomolecular Engineering, University of California, Irvine, Irvine, California 92697, United States

[2]Department of Chemical Engineering, King Fahd University of Petroleum and Minerals, Dhahran, Saudi Arabia

[3]Department of Mechanical Engineering, West Virginia University, West Virginia, United States

[4]Department of Chemical and Environmental Engineering, University of California, Riverside, Riverside, California 92507, United States

[5]Department of Material Science and Engineering, Bourns College of Engineering, University of California, Riverside, Material Science and Engineering Building, 900 University Ave, Riverside, California 92507, United States

1 Abstract

The secondary internal effectiveness factor η_2 in a two-reaction-in-series system (A + B -> C + D, C + B -> E+F) can be above unity for positive-order reaction kinetics. While the controlling factor in the reaction-diffusion phenomenon for the first reaction can be determined using the Weisz criterion based on the value of the primary internal effectiveness factor η_1, the criteria to assign the secondary effectiveness factor that is above unity ($\eta_2 > 1$) do not exist yet, making difficult the development of determinable overall controlling factors in the R_1-R_2-D phenomena in the two-reaction-in-series system. Here, using a two-step methanol oxidation reaction as a case study, we combined an analytically derived criterion for R_1-R_2 phenomenon with the Weisz criterion for R_1-D phenomenon to allow the development of assignment criteria for four overall controlling factors. The overall assignment criteria are found to be dependent on the internal effectiveness factors η_1 and η_2, as well as the rate of the individual reactions at the catalyst surface. When the assignments criteria are re-decomposed using assignable criteria that are based on only η_1 and η_2, a child component criterion is confirmed to satisfy the overall assignment criteria. Based on the sensitivity of the overall controlling factor with respect to the reaction temperature and catalyst size, the selectivity of the formaldehyde intermediate species in methanol oxidation reaction can be enhanced at high reaction temperature when catalysts are specifically designed to enhance the rate

of formaldehyde formation (rate of the first reaction). However, CO formation (the rate of the second reaction) needs to be suppressed to enhance selectivity towards formaldehyde at moderately low temperature. This reaction-diffusion theoretical framework provides guidance for the development of highly selective catalyst for two-reactions-in-series systems and can be extended for higher-number multiple reactions in series and in parallel.

2 Introduction

The internal mass transfer has been considered in a vast number of heterogeneous catalysis studies in different applications ranging from bio-applications [1,2] and biomass upgrading[3] to thermal catalysis [4–8] and energy materials [9–12]. The internal transport effect in porous catalytic materials is studied in a reaction-diffusion phenomenon where it is coupled with the intrinsic kinetics of the catalysts [13]. For single reactions, the reaction-diffusion phenomenon is used to understand and design active catalysts [14]. However, the phenomenon becomes more complex for reactions involving multiple steps, as each of the reactions occurs at a different rate, competing with the diffusion rate of species to a different extent. Consequently, an overall controlling factor for the system emerges, which could be any of the reactions or the diffusion of the species. For example, an overall R_1-R_2-D reactions-diffusion phenomenon occurs in a two-reaction system, in which any of R_1, R_2 or D can be a possible controlling factor. Determining the overall controlling factor in such multiple reactions can be very critical to the understanding and design of highly selective catalysts [15].

Reaction-diffusion phenomenon occurring within a catalyst particle is a complex one that dictates the species' concentration and temperature profiles inside the catalyst. After the development of the model of the phenomenon by Thiele [14] and a similar model by Zeldovich [16] both in 1939, and the invention of the Weisz-Prater criteria in 1954 by Weisz and Prater [17], two parameters - the Thiele modulus and the internal effectiveness factor derivable from the solution of the model have been widely accepted in the field of reaction engineering to characterize the reaction-diffusion phenomena [18] and are in fact currently the state-of-the-art. Infrared microimaging was recently demonstrated as a pioneering experimental one-shot measurement of the internal effectiveness factor for catalytic hydrogenation of benzene to cyclohexane, however, this is still limited to simple kinetics and non-industrial relevant reaction conditions [19]. While the experimental method to investigate reaction-diffusion phenomenon will begin to improve with the potential for new ones to spring up, the reaction-diffusion modelling approach remains more advanced and more widely applied to a variety of reaction systems and conditions [20–22].

The reaction-diffusion phenomena involving single positive-order-kinetics reactions are not only easily determined using the Weisz criteria, but the model solutions are also easy to achieve. Analytical solutions are readily available for models involving single reactions with n-order kinetics [18] occurring in catalysts of different geometries, including spherical, cylindrical, and slab,

and they have been widely applied for different reactions. On the other hand, reaction-diffusion models of single reactions with complex reaction kinetics become more complicated for a solution. Langmuir–Hinshelwood kinetics for single reactant/reaction in isothermal case require certain approximations and simplifications for the development of an analytical solution to determine the internal effectiveness factor for the reaction [23,24]. Also, reaction-diffusion model for a single reaction with a reaction order less than one that results in a large Thiele modulus requires an improved shooting method for numerical solution due to the failure of the conventional shooting method [25].

Apart from increased complexity due to complicated kinetics, the multiplicity of reactions results in complicated reaction-diffusion phenomena with more competing factors; and the resulting models of the phenomena also become very complex for solutions. The primary effectiveness factor for the single reaction is not directly applicable to the subsequent reactions and the Thiele modulus is difficult to derive for multiple reactions due to the simultaneous generation and consumption of the intermediate species [26,27], as well as the complexity of the kinetics involved. Yet, Peters et al. successfully developed an analytical solution for the reaction-diffusion model for two reactions in series A->B->C occurring within a slab in which the secondary effectiveness factor was derived and deployed in a plug flow and stirred batch framework for theoretical prediction of solvent−solid phase partitioning and interior mass transfer limitations in catalytic reactions in series [27]. In his follow-up paper, the analytical solution was extended to spherical and cylindrical geometries [28]. In the same year, a system of reaction-diffusion model equations involving multiple reactions was also solved analytically using eigen analysis by Lattanzi et al [26], with the internal effectiveness factor obtained by integrating the concentration profile using the multistep effectiveness vector (MEV) and DNS. However, Peter's and Lattanzi's analytical solutions were only demonstrated for first order kinetics and isothermal cases, even though the reaction rate in the model solved by Lattanzi et al [26] was additionally considered as a function of temperature through the Arrhenius equation. In addition, effectiveness factors estimated for isothermal cases can be underestimated and overestimated for exothermic and endothermic reactions, respectively, when compared to non-isothermal case estimation [29]. Non-isothermal models generally involve the additional consideration of energy conservation with the mass conservations, in addition to the reaction kinetics in both conservations being considered as functions of temperature through the Arrhenius relation. So far, the non-isothermal models that have been developed and solved either analytically or numerically involve simple kinetics such as n-order kinetics [29–33]. However, with complex kinetics, these models result in systems of differential equations that are highly complex and coupled in both concentrations and temperature, requiring numerical solutions.

Despite the computational cost associated with numerical solutions of complex models, a reaction-diffusion model involving non-isothermal multiple reactions with complex kinetics is a robust model that is applicable to a wide variety of reactions in practical sense without unnecessary assumptions. For such models, Tesser et al. [34] obtained a numerical solution using the method of

lines for a reaction-diffusion model of two reactions-in-series with complex reaction kinetics occurring non-isothermally in a spherical catalyst. The first reaction involving the partial oxidation of methanol to formaldehyde has an inhibition-corrected Mars Van Krevlen rate law with a net positive order while the second reaction involves formaldehyde oxidation to CO and is of pseudo-first order kinetics which is also a positive order kinetics. The internal effectiveness factors of the two reactions were consequently determined in which the secondary internal effectiveness factor is above 1 while the primary internal effectiveness factor is below 1. However, a method to determine the overall controlling factors in the reactions-diffusion R_1-R_2-D phenomena occurring for such two reactions-in-series system is unknown.

In this work, we developed the assignment criteria to identify some derived overall controlling factors in the reactions-diffusion phenomena occurring in a two-step reaction. The developed assignment criteria were validated, and the overall controlling factors were consequently applied to infer selectivity enhancement strategies for the intermediate formaldehyde species in the two reaction-in-series methanol oxidation reaction over iron–molybdenum oxide spherical catalysts.

3 Model development and numerical solution approach

Model development:

The reaction-diffusion phenomenon involving multiple reactions occurring non-isothermally inside the iron–molybdenum oxide spherical catalyst is described by the steady state mass and energy balance of species described by equations (1) and (2) [34], ignoring the convection effects within the catalysts pore since molecules flow into and out of the pores mainly by diffusion [35].

$$Deff_i\left[\frac{d^2C_i}{dr^2}+\frac{2}{r}\frac{dC_i}{dr}\right]=-\rho_p\sum_{j=1}^{N_r}\gamma_{i,j}v_j \qquad i=1,2,\ldots.,Nc.\ \ j=1,..,Nr \quad \ldots\ldots\ldots(1)$$

$$Keff\left[\frac{d^2T_P}{dr^2}+\frac{2}{r}\frac{dT}{dr}\right]=\rho_p\sum_{j=1}^{N_r}(-\Delta H_J)v_j \quad \ldots\ldots\ldots\ldots\ldots\ldots\ldots\ldots\ldots\ldots\ldots\ldots(2)$$

where Nc and Nr are the number of species and number of reactions respectively. The Neumann boundary condition and Dirichlet boundary condition are suitably applicable at the catalyst's center and surface respectively as described in equation 3 and 4 respectively.

$$At\ r=0, \qquad \frac{dC_i}{dr}=0\,, \qquad \frac{dT}{dr}=0 \ldots\ldots\ldots\ldots\ldots\ldots\ldots\ldots\ldots\ldots\ldots\ldots\ldots\ldots \qquad (3)$$

$$At\ r=R_P, \qquad C_i=C_{is}, \qquad T=T_s \ldots\ldots\ldots\ldots\ldots\ldots\ldots\ldots\ldots\ldots\ldots\ldots\ldots\ldots \qquad (4)$$

in which C_i is the concentration of the species inside the catalysts while the Cis is the concentration of each species at the surface and the T_s is the temperature at the catalyst's surface. The concentration of each species is obtained from the total concentration using the mole fraction of the species at the surface. For gas phase, the total concentration at the surface is obtained from the total pressure and temperature of the bulk gas at the surface using $C_S = \frac{P_S}{RT_S}$, in which the reaction occurs at atmospheric pressure (P_s = 1.10 atm).

The methanol oxidation reaction proceeds over the iron–molybdenum oxide catalyst with catalytic partial oxidation of methanol to formaldehyde followed by a side reaction involving formaldehyde oxidation to CO, resulting in two reactions in series as described below. The physical-chemical properties of the catalyst are highlighted in Table 1.

$$CH_3OH + 0.5O_2 \xrightarrow{k_1} CH_2O + H_2O \quad \text{..... (5)}$$

$$CH_2O + 0.5O_2 \xrightarrow{k_2} CO + H_2O \quad \text{..... (6)}$$

The first reaction proceeds by redox mechanism appropriately described by the Mars Van Krevelen mechanism with the inhibition by water formed during reaction accounted for by a Langmuir–Hinshelwood term [34,36], as described by the rate law in equation 7. On the other hand, the second reaction is pseudo-first order with respect to formaldehyde, whose rate of reaction is described in equation 8. All the relevant kinetic parameters in both rate laws are expressed using the Arrhenius equations as detailed in Table 2.

$$v_1 = \frac{k_1\, k_2\, P_m\, P_{O2}^{0.5}}{k_1\, P_m + k_2 P_{O2}^{0.5}} \left(\frac{1}{1 + b_W\, P_W}\right) \text{.....(7)}$$

$$v_2 = k_3 P_f \text{.....(8)}$$

Using air for the oxidation reaction brings nitrogen into the system resulting in 6 species $CH_3OH, CH_2O, CO, O_2, H_2O, N_2$. The partial pressures of each of the species inside the catalyst are related to their respective concentrations using the ideal equation of state while the concentration of each species is obtained from the total concentration using the mole fraction of the species. Thus, the pressure terms in the rate laws are simplified using $P_i = C_i\, R\, T$; where i is m, O_2, w and f representing methanol, oxygen, water and formaldehyde respectively.

Table 1: Physical-chemical data for gases and methanol oxidation catalyst [34]

Parameters	Values
ρ_p	1000 kg/m^3
Deff	1.07 x 10^{-5} exp(-972/T) m^2/s
Keff	2.72 x 10^{-4} KJ/s m K

Table 2: Kinetic Parameters for the rate laws [34]

k_1	= exp(-18.4586 + 64790/RT)
k_2	= exp(-15.2687+57266/RT)
k_3	= exp(-30.6936+57266/RT)
B_w	= exp(+21.2814 – 111600/RT)
ΔH_1	= 158.8 kJ/mol
ΔH_2	= 238.3 kJ/mol

Finite difference numerical solution:

Applying the steady state mass balance to the six species together with the energy balance results in a set of one-dimensional boundary value problems consisting of seven coupled second order ODEs with fourteen boundary conditions. The ODES are coupled in terms of concentration and temperature.

$$Deff_m \left[\frac{d^2C_m}{dr^2} + \frac{2}{r}\frac{dC_m}{dr}\right] = \rho_p v_1$$

$$Deff_{O2} \left[\frac{d^2C_{O2}}{dr^2} + \frac{2}{r}\frac{dC_{O2}}{dr}\right] = \frac{\rho_p(v_1 + v_2)}{2}$$

$$Deff_f \left[\frac{d^2C_f}{dr^2} + \frac{2}{r}\frac{dC_f}{dr}\right] = \rho_p(-v_1 + v_2)$$

$$Deff_C\left[\frac{d^2C_C}{dr^2}+\frac{2}{r}\frac{dC_C}{dr}\right]=-\rho_p v_2$$

$$Deff\left[\frac{d^2C_W}{dr^2}+\frac{2}{r}\frac{dC_W}{dr}\right]=-\rho_p(v_1+v_2)$$

$$Deff\left[\frac{d^2C_N}{dr^2}+\frac{2}{r}\frac{dC_N}{dr}\right]=0$$

$$Keff\left[\frac{d^2T}{dr^2}+\frac{2}{r}\frac{dT}{dr}\right]=-\rho_p((\Delta H_1)\,v_1+(\Delta H_2)\,v_2)$$

As a demonstration of another numerical solution method other than the method of lines in used by Tesser et al [34], finite difference method was adopted. First, the seven coupled second-order ODEs constituting the reaction-diffusion model were reduced to fourteen (14) coupled first order ODEs, which were consequently transformed to nonlinear algebraic equations using the forward and backward finite difference method. Particle radius discretization using internal points $N_n = 50$ results in a system of 700 coupled nonlinear algebraic equations which were solved in MATLAB using the fsolve function. At 573 K and with surface concentration of 8.0, 16.0, 1.0, 0.0, 0.0, 75.0 % for the $CH_3OH, O_2, CH_2O, CO, H_2O, N2$ species respectively, the solution of the model shows that, due to the exothermicity of the reaction, the temperature increases from the surface into the interior of the catalyst's particle with a maximum temperature difference of about ~3.5 K. As expected, the concentrations of the reactants generally decrease monotonously into the catalysts particle while the product concentration increases monotonously. With respect to the surface concentration of the species, there is a maximum change in concentration by ~ -7.7, -4, 8, 0, 8 % for the $CH_3OH, O_2, CH_2O, CO, H_2O$ species respectively at the center of the catalyst particle, approximately matching with the solution obtained by Tesser et al [34] with the method of lines.

Internal effectiveness factor:

Using the solution of concentration and temperature profiles inside the spherical catalyst, the internal effectiveness factor characterizing the reaction-diffusion phenomenon is determined using equation 9

$$\eta_j=\frac{\int_0^{Rp}4\pi r^2 v_j(C_i,T)dr}{\left(\frac{4}{3}\right)\pi Rp^3 v_j\left(C_i^s,T_s\right)}\;;where\quad \text{j = 1,2 for reaction 1 and 2}\qquad \ldots\ldots\ldots\ldots\qquad (9)$$

It should be noted that the internal effectiveness factor is influenced by the degree of the uniformity of the species concentration and temperature inside the catalysts with respect to surface species concentration and temperature.

4 Results and Discussion

4.1 Dependence of controlling factor of individual reaction-diffusion phenomena on reaction temperature and catalyst size

The reaction-diffusion model for the non-isothermal two-reaction-in-series system with complex kinetics was solved for methanol oxidation reaction over the iron-molybdenum catalyst using the finite difference method. Figure 1 shows that the concentration and temperature profiles inside spherical catalysts have different degrees of gradient depending on the catalyst size and reaction temperature. For a 100 μm catalyst particle size at 500 K, there is a noticeable gradient in the concentration of all species and temperature inside the catalysts - the species have a maximum percentage concentration change of ~ -4, -2, 5, 0, 4 % at the center of the catalyst particle with respect to the surface concentration of 8.0, 16.0, 1.0, 0.0, 0.0, for $CH_3OH, O_2, CH_2O, CO, H_2O$ respectively, and a maximum temperature change of 1.8 K at the center of the catalyst particle with respect to the catalysts surface temperature. As the catalyst size reduces to 10 μm and further to 500 nm, the maximum change in each species concentration and temperature becomes reduced, indicating enhanced uniformity of concentration and temperature within the catalyst's particle. In addition to increased uniformity at reduced particle size, the uniformity of the concentration and temperature of species inside the spherical catalyst is also enhanced as the temperature is increased from 500 K to 800 K for the three particle sizes. Based on the definition of internal effectiveness factor η described in equation 9, the increased uniformity of temperature and concentration of species is expected to drive the internal effectiveness factors for the two reactions towards 1. This is consistent with the increase and decrease of the internal effectiveness factor η_1 and η_2 for reaction 1 and reaction 2 respectively towards 1 caused by the reduced catalysts size and enhanced temperature shown in Figure *2*. However, the surface temperature can also influence the surface reactions, causing a direct influence on the internal effectiveness factor. The indirect effect of reaction temperature (through enhanced temperature inside the catalysts particle) and the direct effect of temperature on the primary internal effectiveness factor could be competitive, resulting in the sinusoidal behavior of the $\eta_1 - \mathrm{T}$ profile as the temperature is increased, as observed in Figure 2c. It seems that the dominance of the direct temperature effect (through the reaction rate) over the indirect effect (through concentration and temperature gradient) is more pronounced at high catalyst size causing the low value of η_1 even at high temperature.

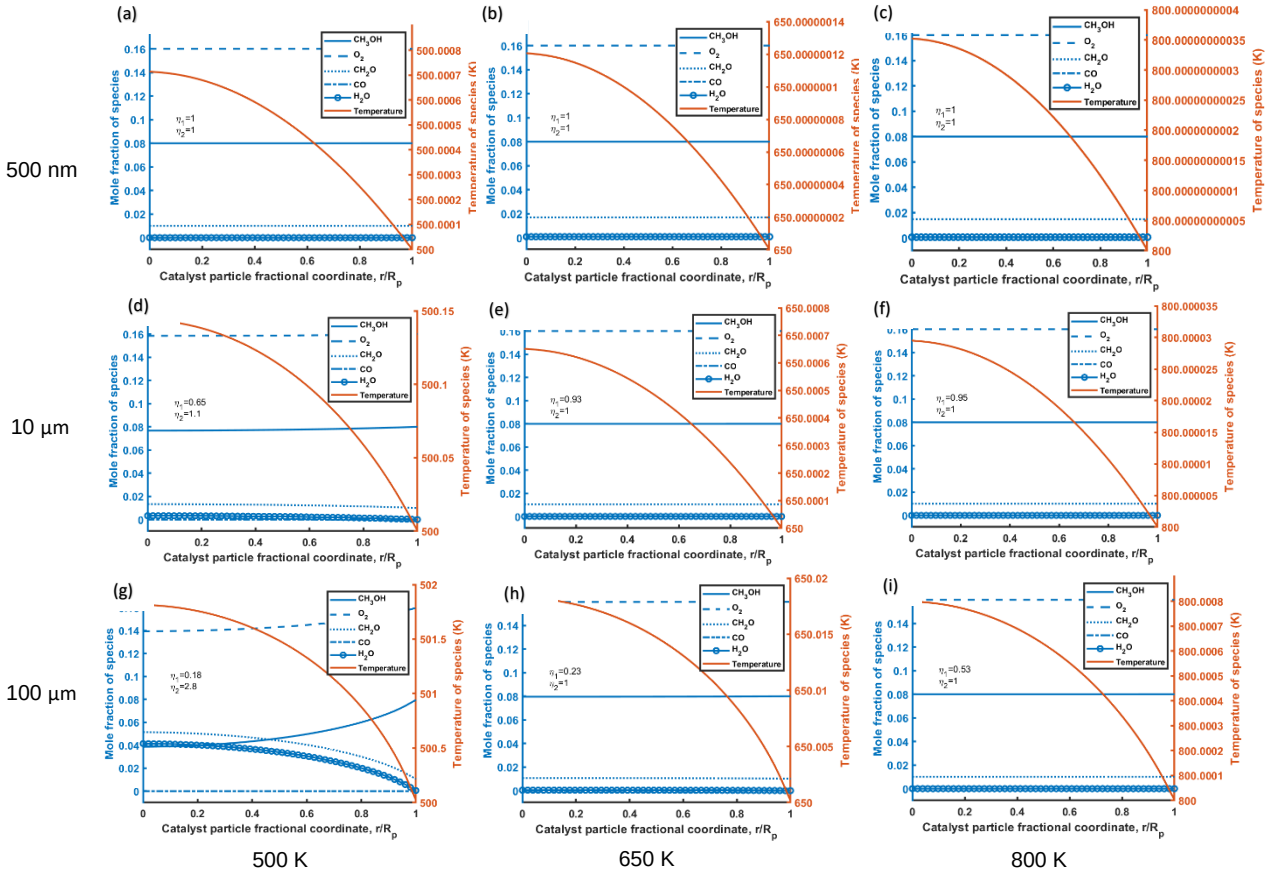

Figure 1: (a) – (i) Effect of catalyst size and temperature on species concentration and temperature profile inside spherical catalyst. The significant figures of the temperature have been deliberately left higher to show the direction of change of the temperature inside the catalyst's particle. The temperature increases into the center of the catalyst particle. C_s = 8.0, 16.0, 1.0, 0.0, 0.0, 75.0 % for $CH_3OH, O_2, CH_2O, CO, H_2O, N_2$ respectively

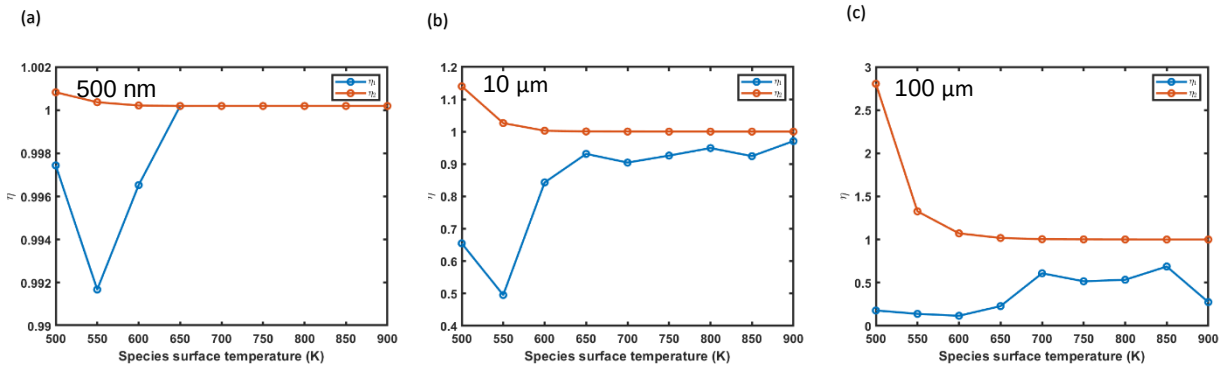

Figure 2: Effect of catalysts particle size and temperature on the primary and secondary internal effectiveness factors. Cs = 8.0, 16.0, 1.0, 0.0, 0.0, 75.0 for $CH_3OH, O_2, CH_2O, CO, H_2O, N_2$ respectively

However, more specifically, catalyst size reduction and temperature enhancement cause the increase of $\eta_1$towards 1 with a maximum possible value of 1, while the η_2 decreases towards 1, with 1 being its minimum possible value. The rate of the reaction 1 is maximum at the catalyst surface since the reactant concentration decreases into the interior of the catalysts, leading to a maximum possible value of 1 for the η_1. The maximum value of unity as an upper bound for η_1 implies the equality of the reaction rate inside the catalysts and that at the catalyst surface, indicating a perfect situation of reaction 1 dominating with no resisting contribution from the species' diffusion. For such unity upper-bounded η, Weisz criteria [23] stipulate an assignment of $\eta > 0.95$ for control by reaction and $\eta < 0.95$ for diffusion controlling. On the other hand, the rate of reaction 2 is maximum inside the catalyst due to the increasing concentration of the formaldehyde intermediate into the interior of the catalysts, leading to the η_2 value to be always above 1. In consistence with the definition of internal effectiveness factor, when η_2 is at its minimum value of 1, the reaction rate inside the catalysts is the same as that at the surface, indicating the perfect condition of reaction 2 controlling with respect to diffusion (as indicated by the 500 μm and 800 K with uniform concentration and relatively uniform temperature profile). A critical value x should therefore exist (such that x>1) at which the control by reaction 2 begins, with η_2 above this x value indicating the control by diffusion with respect to reaction 2. While Weisz stipulates the critical value of 0.95 for unity upper-bounded η such as in the case of η_1, there exists no such critical value x for unity lower-bounded η (η greater than 1) as in the case of η_2, only a special case of $\eta_2 = 1$ where reaction 2 absolutely controls, can be determined.

Based on Weisz criteria for reaction 1 ($\eta_1 < 0.95$ for reaction controlling or $\eta_1 > 0.95$ for diffusion controlling) and the ($\eta_2 = 1$) criteria for perfect condition of reaction 2 controlling, the effects of temperature and catalyst size on the reaction-diffusion phenomena for the two individual reactions can be determined using the internal effectiveness factors for the two reactions. For 500 nm catalyst size considered between 500 K to 900 K, reaction 1 controls in this temperature range since η_1 remains above 0.95 in the range as shown in Figure 2. In addition, the potential for the perfect control of reaction 1 to dominate is enhanced with increased temperature due to the increasing η_1. On the other hand, the perfect condition of reaction 2 controlling begins from about 600 K and beyond as indicated by the onset of η_2 achieving its minimum value of 1 from this temperature. As the catalyst size increases to 10 μm, increasing temperature also enhances the potential for control by reaction 1 and reaction 2. However, the potential for both reactions to control becomes retarded as the temperature to achieve the reaction 1 controlling becomes increased compared to those of 500 nm, in ditto to reaction 2 controlling whose perfect reaction 2 control increases to about 700 K. With further increase in catalysts size to 100- μm, perfect reaction 2 controlling begins at a much higher temperature (800 K) while reaction 1 does not control with respect to diffusion even at 900 ^{o}C. This directly implies that, while the temperature generally increases reaction control, the catalyst size decreases its potential. Invariably, both reactions individually control with respect to diffusion with a small catalyst size, which is consistent with the reported occurrence of diffusion-limitation in larger particle size [26]. However, based on the control of reaction 1 and the perfect condition of reaction 2 ($\eta_2 = 1$ criteria), the suppression of

the reaction controlling for increasing catalyst size is more dominant on reaction 1 than on reaction 2.

4.2 Development of assignment criteria for the overall controlling factor in two series reactions

With known internal effectiveness factors for two reactions in series, the two possible individual controlling factors in the reaction-diffusion phenomena for each reaction can be combined to form four overall controlling factors $R_1<D$, $R_2<D$; $R_1<D<R_2$; $R_2<D<R_1$; and $D<R_1$, $D<R_2$, as shown in Table 3. The corresponding overall assignment criteria for the four overall controlling factors can be defined in terms of the individual η_1 and η_2 values as highlighted in Table 4 by combining the corresponding criteria for the two possible factors for each of the two reaction-diffusion phenomena. However, the combined overall assignment criteria in Table 4 cannot be applied since the critical x value for the η_2 is unknown for reaction 2. Hence, an alternative approach is innovated to develop some overall controlling factors whose assignment criteria can be determined and applied.

Table 3: Overall controlling factor obtained by combining the individual controlling factors for $R_1<D$ and $R_2<D$

	$R_1<D$	$D<R_1$
$R_2<D$	$R_1<D$, $R_2<D$	$R_2<D<R_1$
$D<R_2$	$R_1<D<R_2$	$D<R_1$, $D<R_2$

Table 4: Criteria based on η_1 and η_2– but the assignment cannot be made since there is no eta assignment criteria for $R_2<D$ (and $D<R_2$)

	Overall Controlling factors	η_1 condition (Weisz criteria)	η_2 criteria
A1	$R_1<D$, $R_2<D$	$1 \geq \eta_1 > 0.95$	$1 \leq \eta_2 < x$
A2	$R_1<D<R_2$	$1 \geq \eta_1 > 0.95$	$\eta_2 > x$
A3	$R_2<D<R_1$	$\eta_1 < 0.95$	$1 \leq \eta_2 < x$
A4	$D<R_1$, $D<R_2$	$\eta_1 < 0.95$	$\eta_2 > x$

Due to the lack of the criteria to assign η_2 (for the R_2-D phenomena), the relative rate of the two reactions (R_1-R_2) is considered and combined with the R_1-D phenomena (since it can be assigned by the Weisz criteria), resulting in four overall controlling factors for the two reactions, as shown

in Table 5. First, the criteria for assigning controlling factor in R_1-R_2 phenomenon that allows the determination of the relative importance of reaction 1 with respect to reaction 2 is derived as follows. For reaction 1 controlling with respect to reaction 2, the sum rate of reaction 1 is less than the sum rate of reaction 2 since the controlling step is the determining step. Hence equation (11) holds.

$$\int_0^{Rp} 4\pi r^2 \rho v_1(C_i, Tp)dr < \int_0^{Rp} 4\pi r^2 \rho v_2(C_i, T)dr \ldots\ldots\ldots\ldots\ldots\ldots\ldots\ldots\ldots\ldots\ldots\ldots . (11)$$

Since the definition of η is general irrespective of its bounds, equation (12) can be obtained by recurring equation (9)

$$\eta_1 \left(\frac{4}{3}\right)\pi {R_p}^3 v_1(C_i^s, T_s) < \eta_2 \left(\frac{4}{3}\right)\pi {R_p}^3 v_2(C_i^s, T_s) \ldots\ldots\ldots\ldots\ldots\ldots\ldots\ldots\ldots\ldots\ldots . (12)$$

And further simplification leads to

$$\eta_1 {R_p}^3 v_1(C_i^s, T_s) < \eta_2 \, {R_p}^3 v_2(C_i^s, T_s) \ldots\ldots\ldots\ldots\ldots\ldots\ldots\ldots\ldots\ldots\ldots\ldots\ldots\ldots\ldots . (13)$$

Since the R-D phenomenon occurs in the same catalyst of radius R_p, equation (13) leads to equation (14)

$$\eta_1 v_1(C_i^s, T_s) < \eta_2 \, v_2(C_i^s, T_s) \ldots\ldots\ldots\ldots\ldots\ldots\ldots\ldots\ldots\ldots\ldots\ldots\ldots\ldots\ldots\ldots . (14)$$

An auxiliary of equation (14) is equation (15)

$$v_1(C_i^s, T_s) < v_2(C_i^s, T_s) \;\; iff \; \eta_1 < \eta_2 \ldots\ldots\ldots\ldots\ldots\ldots\ldots\ldots\ldots\ldots\ldots\ldots\ldots\ldots\ldots\ldots . (15)$$

According to equation (15), for reaction 1 to control with respect to reaction 2, the η_1 should be less than η_2 in addition to the surface rate of reaction 1 being less than the surface rate of reaction 2. This implies that comparisons of surface reaction rates and internal effectiveness factors need to be considered for the assignment criteria. In other words, neither only the surface reaction rates nor only the internal effectiveness factor for the individual reactions will be sufficient to determine the relative controlling factor between the two reactions. Hence, equation (14) which is more general and defined in terms of the η_1 and η_2 and the surface reaction rates becomes a general criterion to determine the relative importance of reaction 1 with respect to reaction 2. While

equation (14) specifically holds for when reaction 1 controls with respect to reaction 2 (R_1/R_2), its reverse also holds when reaction 2 controls with respect to reaction 1 (R_2/R_1).

Combining the derived criteria for the relative rates of the two reactions (R_1-R_2 phenomena) with the Weisz criteria for reaction 1 (R_1-D) result in the overall assignment criteria highlighted in Table 6 for the developed four overall controlling regions $R_1<R_2$, $R_1<D$; $D<R_1<R_2$; $R_2<R_1<D$; $R_2<R_1$, $D<R_1$ given in Table 5. Both the R_1-R_2 criteria and the R_1-D Weisz criteria must be satisfied to obtain each of the overall controlling regions; for example, both $\eta_1 > 0.95$ and $\eta_1 v_1(C_i^s, T_s) < \eta_2\ v_2(C_i^s, T_s)$ must be satisfied for the $R_1< R_2$, $R_1< D$ to be achieved. These criteria can be easily applied after obtaining the solution of the reaction-diffusion model and the internal effectiveness factors.

Table 5: Controlling factors developed based on the combination of R_1-D and R_1-R_2 phenomena.

	$R_2<R_1$	$R_1<R_2$
$D<R_1$	$R_2<R_1$, $D<R_1$	$D<R_1<R_2$
$R_1<D$	$R_2<R_1<D$	$R_1<R_2$, $R_1<D$

Table 6: Assignment criteria for controlling regions developed by combining the R_1-D and R_1-R_2 phenomena.

	Overall controlling factors	$\eta_1$condition (Weisz criteria)	Developed criteria $v_1\ vs\ v_2\ conditions$
B1	$R_2<R_1$, $D<R_1$	$\eta_1 < 0.95$	$\eta_1 v_1(C_i^s, T_s) > \eta_2\ v_2(C_i^s, T_s)$
B2	$D<R_1<R_2$	$\eta_1 < 0.95$	$\eta_1 v_1(C_i^s, T_s) < \eta_2\ v_2(C_i^s, T_s)$
B3	$R_2<R_1<D$	$\eta_1 > 0.95$	$\eta_1 v_1(C_i^s, T_s) > \eta_2\ v_2(C_i^s, T_s)$
B4	$R_1< R_2$, $R_1< D$	$\eta_1 > 0.95$	$\eta_1 v_1(C_i^s, T_s) < \eta_2\ v_2(C_i^s, T_s)$

Hence, based on rate limiting step as being the controlling factor, the overall controlling factor $R_1< R_2$, $R_1< D$ implies that R_1 controls in the overall R_1-R_2-D phenomenon, while diffusion controls overall for $D<R_1<R_2$. The $R_2<R_1<D$ indicates that R_2 controls overall. However, for $R_1< R_2$, $R_1< D$ region, either R_2 or D controls the phenomenon overall, as it is difficult to determine the overall control unless the relative control between the R_2 and D (that is, η_2) is known.

Validation of the developed overall assignment criteria: The overall assignment criteria for R_1-R_2-D phenomena developed by combining the Weisz criteria of R_1/D and the derived R_1/R_2 criteria are validated using the combination of the known R_1-D criteria ($\eta_1 < 0.95$; or $\eta_1 > 0.95$) and the known R_2-D criteria only, i.e based on the combination of η_1 and η_2. Due to the non-availability

of critical x value for η_2, only the perfect condition of reaction 2 ($\eta_2 = 1$) is considered in the R_2-D phenomena used for the validation. The validation is approached by first decomposing the developed overall regions highlighted in Table 6 into child components where possible. As shown in Figure *3* a, $D<R_1<R_2$ which is $D<R_1$, $D<R_2$, $R_1<R_2$ cannot be assigned using only η_1 and η_2 due to the additional $R_1<R_2$. Similarly, $R_2<R_1<D$ which is $R_2<D$, $R_1<D$, $R_2<R_1$ cannot also be assigned by only η_1 and η_2 due to the additional $R_2<R_1$. Although B4 ($R_1< R_2$, $R_1< D$) can be decomposed into $R_1<D<R_2$ and $R_1<R_2<D$ as shown in Figure 4, the $R_1<R_2<D$ which is essentially $R_1<D$, $R_2<D$ and $R_1<R_2$ cannot be assigned using only η_1 and η_2 due to the additional $R_1<R_2$ while the combined assignment for $R_1<D<R_2$ using η_1 and $\eta_2 > x$ cannot be determined due to the unavailability of the critical x value.

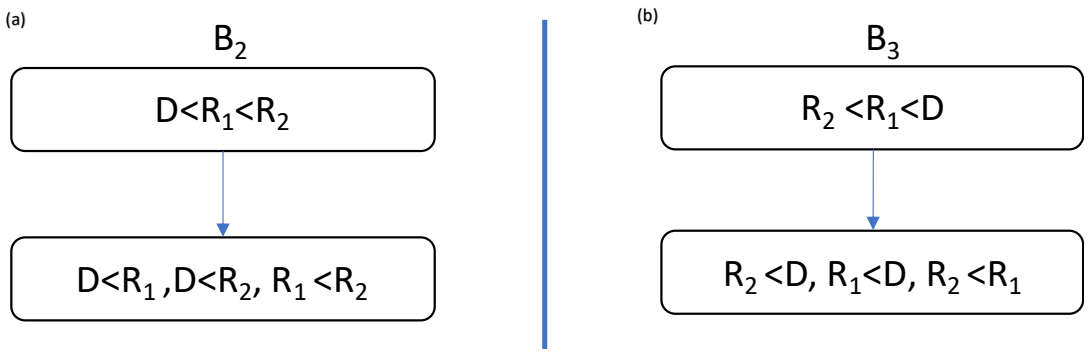

Figure 3: Analogy for the decomposition of B_2 ($D<R_1<R_2$) and B_3 ($R_2<R_1<D$) regions

As shown in Figure *5*, the overall controlling factor B_1 ($R_2<R_1$, $D<R$) can be decomposed into ($D<R_2<R_1$) and ($R_2<D<R_1$). The $D<R_2<R_1$ which is essentially $D<R_2$, $D<R_1$, $R_2<R_1$ cannot be assigned using only η_1 and η_2 due to the additional $R_2<R_1$ criteria.

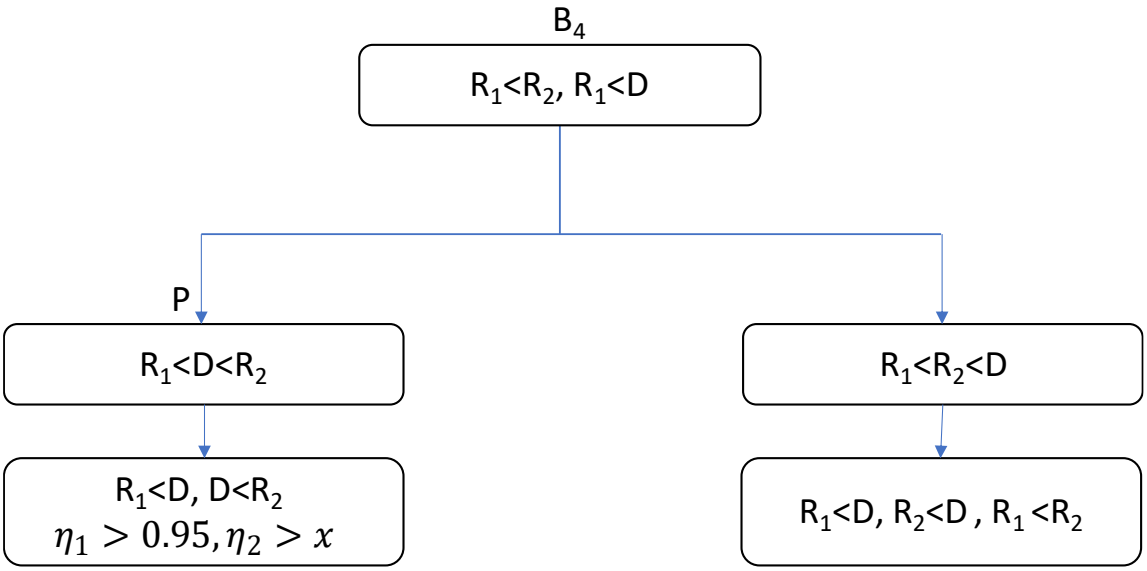

Figure 4: Analogy for the decomposition of B_4 ($R_1<R_2$, $R_1<D$) region

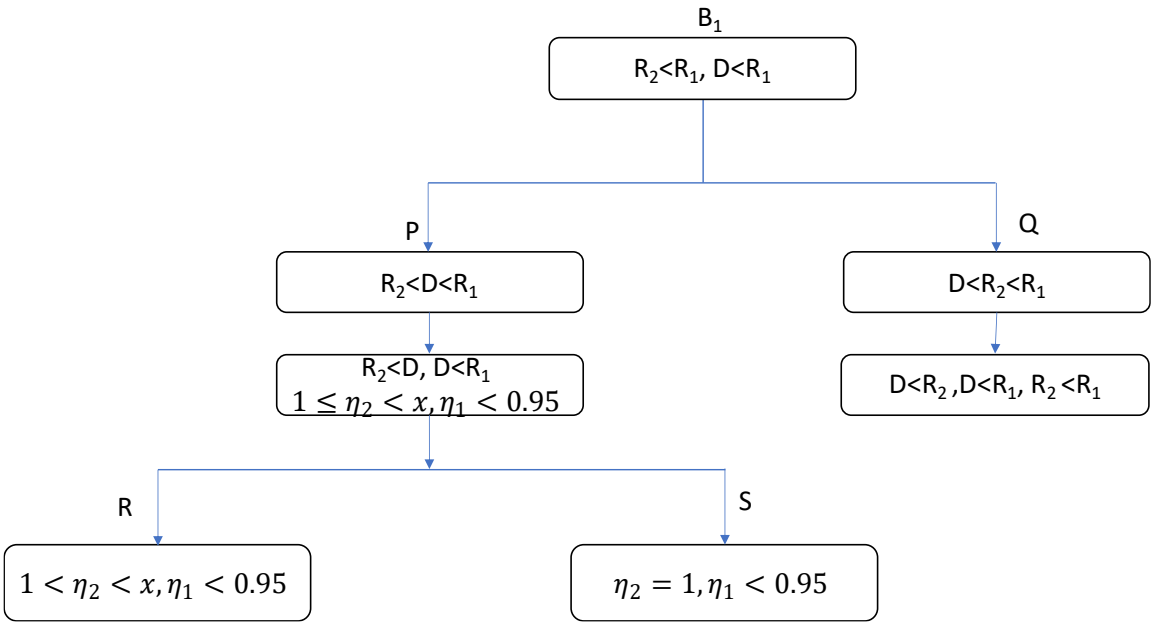

Figure 5: Analogy for the decomposition of B_1 ($R_2<R_1$, $D<R$) region

However, R_2<D<R_1, which is essentially R_2<D, D<R_1 has assignment criteria of $1 \leq \eta_2 < x$ and $\eta_1 < 0.95$ that can be further decomposed into $1 < \eta_2 < x$, $\eta_1 < 0.95$ and $\eta_2 = 1$, $\eta_1 < 0.95$. While the criteria $1 < \eta_2 < x, \eta_1 < 0.95$ cannot be applied due to the non-availability of critical x value, the $\eta_2 = 1, \eta_1 < 0.95$ can be applied using only the values of η_1 and η_2. Consequently, the region (say S) determined by the $\eta_2 = 1, \eta_1 < 0.95$ criteria should be a subset of the decomposed parent (overall controlling) region B_1 (R_2<R_1, D<R) which can be determined by the derived criteria $\eta_1 < 0.95$, $\eta_1 v_1(C_i^s, T_s) > \eta_2\, v_2(C_i^s, T_s)$ as shown in Table *6*, i.e. S ⊆ B_1. This also directly implies that the $\eta_2 = 1, \eta_1 < 0.95$ criteria satisfy the parent criteria $\eta_1 < 0.95$, $\eta_1 v_1(C_i^s, T_s) > \eta_2\, v_2(C_i^s, T_s)$. For the satisfaction to hold,

Substituting $\eta_2 = 1$ in $\eta_1 v_1(C_i^s, T_s) > \eta_2\, v_2(C_i^s, T_s)$ yields,

$$\eta_1 v_1(C_i^s, T_s) > v_2(C_i^s, T_s)$$

$$\eta_1 > \frac{v_2(C_i^s, T_s)}{v_1(C_i^s, T_s)}$$

Considering $\eta_1 < 0.95$,

$$0.95 > \eta_1 > \frac{v_2(C_i^s, T_s)}{v_1(C_i^s, T_s)}$$

$$\frac{v_2(C_i^s, T_s)}{v_1(C_i^s, T_s)} < 0.95$$

While the $\eta_2 = 1, \eta_1 < 0.95$ criteria as a subset of the parent criteria $\eta_1 < 0.95$, $\eta_1 v_1(C_i^s, T_s) > \eta_2\, v_2(C_i^s, T_s)$ can be considered a necessary condition to validate the overall region R_2<R_1, D<R and the corresponding derived assignment criteria, we consider the $\frac{v_2(C_i^s, T_s)}{v_1(C_i^s, T_s)} < 0.95$ criterion as an additional and sufficient criterion for the confirmation of the validation of the overall controlling region B_1 (R_2<R_1, D<R) in Table 6. Figure 6 shows the η_1-T and η_2-T plots for catalysts size of 500- μm with temperature ranging from 500-1000 K and C_s = [0.08, 0.16, 0.01, 0, 0, 0.75]. Only the R_2<R_1, D<R_1 region occurs within the whole 500 – 1000 K temperature range considered, while a region (called $R_2R_1DR_1$ case study) assigned by $\eta_2 = 1, \eta_1 < 0.95$ occurs from 775 to 1000 K, which is within the 500 – 1000 K temperature range of R_2<R_1, D<R_1. In addition, $\frac{v_2(C_i^s, T_s)}{v_1(C_i^s, T_s)}$ remains less than 0.95 within the 775 to 1000 K temperature range occupied by the $R_2R_1DR_1$ case study.

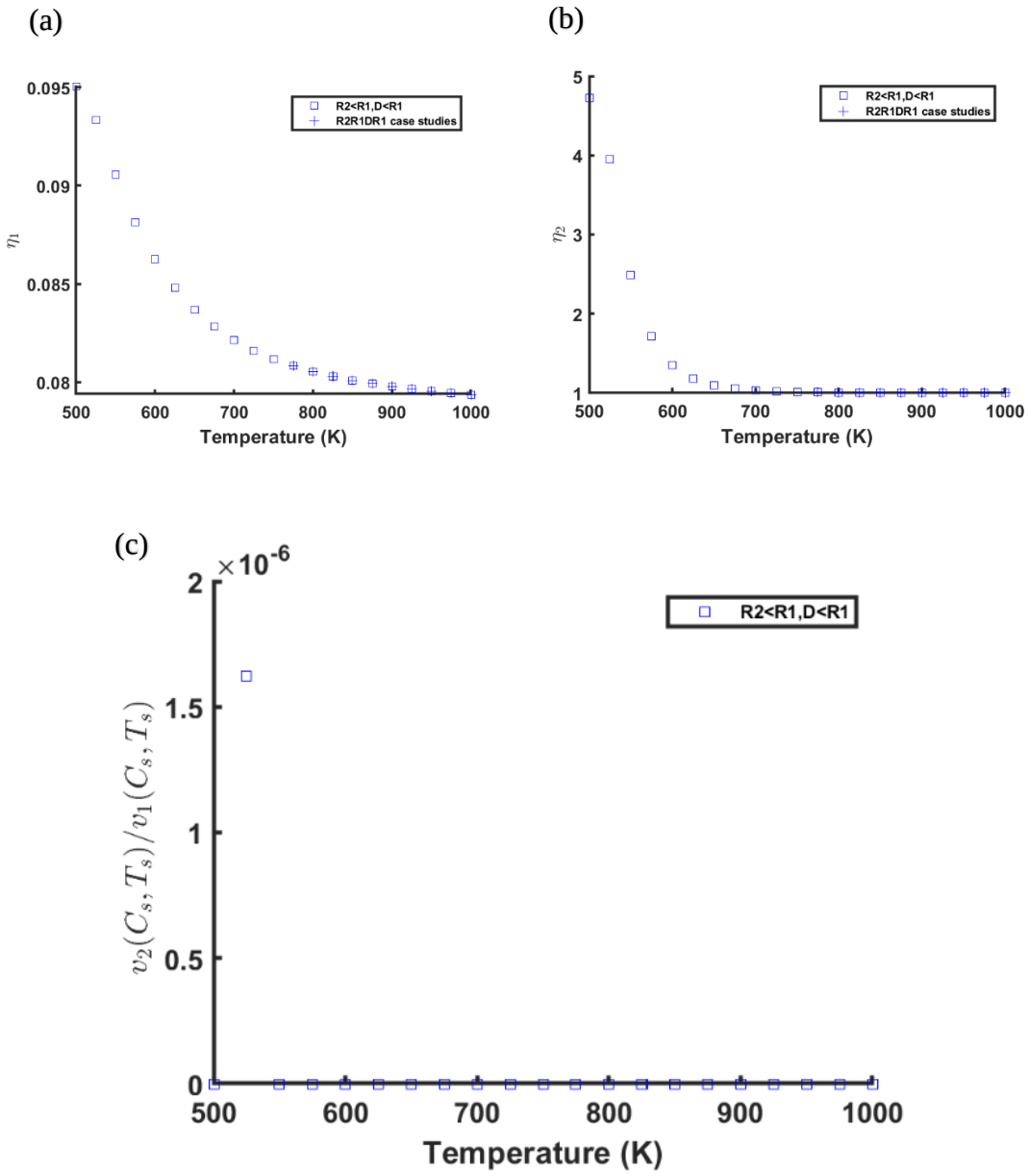

Figure 6: The (a) η_1-T and (b) η_2-T curves for catalyst size 500- μm , 500-1000 K temperature range (500:25:1000). The R_2<R_1, D<R_1 is assigned using the derived criteria (combination of $\eta_1 < 0.95$ and $\eta_1 v_1(C_i^s, T_s) > \eta_2\ v_2(C_i^s, T_s)$) while the R2R1DR1 case study is assigned using the validated criteria (combination of $\eta_2 = 1\ and\ \eta_1 < 0.95$) (c) $v_2(C_i^s, T_s)/v_1(C_i^s, T_s)$ vs Temperature for the same conditions

4.3 Enhancement strategy for intermediate species selectivity in two-reactions-in-series

The overall controlling factor in the two-reaction-in-series methanol oxidation reaction is determined as a function of the reaction temperature and the catalyst particle size for the design of strategies to enhance the selectivity of the intermediate formaldehyde selectivity. Figure 6a and b show the η_1-T-R_p and η_2-T-R_p curves for catalyst particle size from 50 nm to 500 μm and reaction temperature between 500 to 800 K. Clearly, reaction 1 controls with respect to diffusion at high temperature (η_1 > 0.95) but diffusion begins to control at low temperature as the catalysts size increases. Reaction 2 also controls at high temperature (η_2~1), but the η_2 significantly increases above 1 at low temperature and as the catalyst size increases, indicative of an increasing tendency for diffusion control. However, based on the corresponding 2D map in Figure 6c, the overall control by reaction 1 (R_1<R_2, R_1<D region) occurs from 750 K and above, while the overall control by reaction 2 (R_2<R_1<D region) occurs between 550 K and 725 K across all the catalysts sizes. There is a transition from overall control by reaction 2 (R_2<R_1<D region) to overall control by either reaction 2 or diffusion (R_2<R_1, D<R_1 region) at 50 μm catalyst size and 500 K; 150 μm and 525 K; and 370 μm and 550 K. As the temperature further increases from 575 K to 725 K, overall control by reaction 2 (R_2<R_1<D region) begins to set in for the entire catalyst sizes (between 50 nm and 500 μm) considered. This implies that increasing the temperature drives the overall controlling factor from either reaction 2 or diffusion (R_2<R_1, D<R_1) to overall control by reaction 2 (R_2<R_2<D) to overall control by reaction 1 (R_1<R_2, R_1<D), indicating that increased temperature enhances the tendency for the overall reaction to be controlled by reaction 1. This is consistent with the result obtained in section 4.1 in which increasing temperature enhances the potential for control by the individual reactions. Similarly, at low temperature, increasing the catalyst size changes the overall controlling factor from reaction 2 to either reaction 2 or diffusion but this tendency for change fades away as the temperature is increased. This change of the overall controlling factor towards diffusion controlling with increasing catalyst size is also very consistent with the suppression of reactions controlling highlighted in section 4.1 above for large catalysts size.

Since the instantaneous selectivity of an intermediate species in a two-reaction in series is dictated by the ratio of the rate of the reaction of the first reaction to that of the second reaction [18,35], the selectivity of the formaldehyde intermediate species can be improved by either enhancing the rate of reaction 1 or lowering the rate of reaction 2 or combination of both. Hence, above 725 K at which the reaction 1 controls the overall phenomena, increasing the rate of reaction 1 is expected to increase the selectivity towards formaldehyde while increasing the rate of reaction 2 or the diffusion should not cause any increase in formaldehyde selectivity. For temperature between 550 and 725 K where reaction 2 controls overall, selectivity towards formaldehyde can be enhanced by suppressing the rate of reaction 2 while increasing the rate of reaction 1 should not enhance

formaldehyde selectivity. However, at temperature below 550 K for some catalysts' sizes at which diffusion or reaction 2 controls overall ($R_2<R_1$, $D<R_1$), the rate of reaction 2 could be suppressed to improve formaldehyde selectivity, provided the second reaction controls with respect to diffusion.

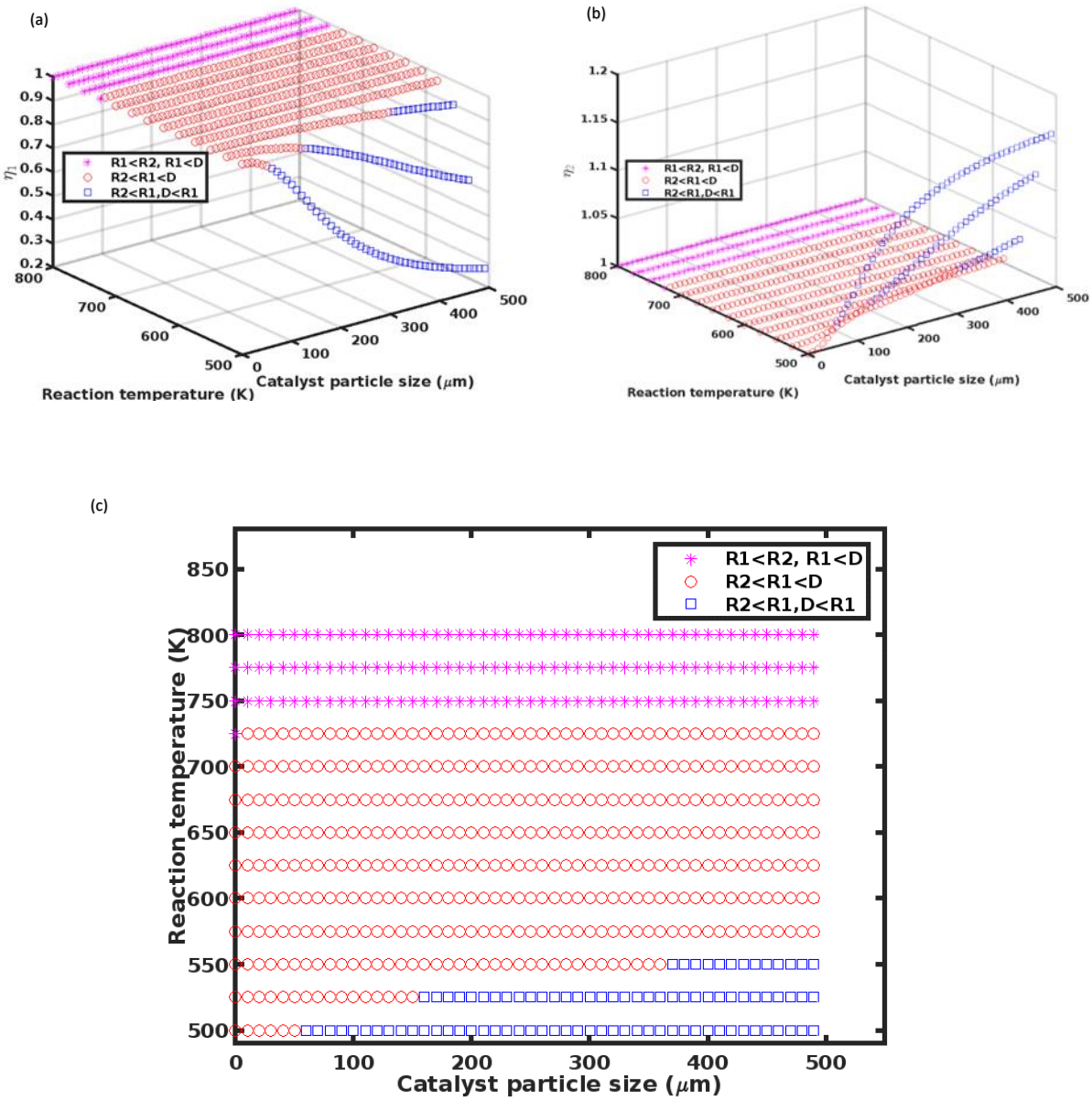

Figure 7: (a) η_1-T-R_p 3D plot (b) η_2-T-R_p 3D plot of catalysts size between 50 nm to 500 μm and temperature between 500 to 800 K (c) 2 D map showing the different controlling factors with respect to the catalysts size and reaction temperature

The rate of the individual reactions in the two reactions-in-series methanol oxidation reaction over iron–molybdenum oxide catalyst is influenced by the chemical composition of the base catalysts, catalyst structure, synthesis technique, synthesis conditions, and promoters, among other factors. The catalytic activity of Mo-Fe-O mixed oxide catalyst is greatly dictated by the Mo/Fe ratio - the activity is enhanced at an optimal Mo/Fe ratio such as Mo/Fe ratio of 1.7 [37], Mo/(Fe+Mo) ratio of 0.75[38], Mo/(Fe+Mo) ratio of 0.802 corresponding to Mo/Fe of 2.4 [39], with the industrial Mo/Fe ratio ranging between 2.3 and 5 [40]. In addition, Mo-rich surface layers that increase the activity of the catalyst can be facilitated by calcining iron molybdates at moderate treatments such as 530–820 K for at least 18 h [41]. It has also been reported that, while methanol oxidation can proceed to formaldehyde on the Fe_3O_4 (001), the reaction can be enhanced by the addition of single Pd atoms, which lowers the barrier to C–H bond cleavage by a factor of 2, leading to formaldehyde desorption [42]. On the other hand, high CO selectivity can be obtained at 350 ^oC calcination, which causes an onset of bulk diffusion [43]. Hence, based on our results, we, therefore, propose that catalysts containing the maximum Mo/Fe ratio or Mo-rich layer or single atoms Pd or other rate enhancement factor for reaction 1 will have enhanced selectivity towards formaldehyde at high reaction temperature. On the other hand, catalysts having enhanced bulk diffusion, or some other reaction 2 enhancement factor can only have enhanced formaldehyde selectivity at a moderate temperature. At extremely low temperatures and relatively larger catalysts size, either suppressing CO or suppressing the diffusion rate could enhance the selectivity depending on the controlling factor in the second reaction.

5 Conclusion

The assignment criteria for the overall controlling factors in the R_1-R_2-D reactions-diffusion phenomena occurring in a two reaction-in series system are developed, validated, and applied. For methanol oxidation reaction occurring as two main reactions in series over iron–molybdenum oxide catalyst, the rates of the individual reactions are generally enhanced by temperature while they are suppressed by large particle-size catalysts. However, the tendency for reaction 1 to control overall increases with increasing temperature and reducing catalyst particle size. Consequently, selectivity of the intermediate formaldehyde can be enhanced at high temperature by increasing the rate of the first reaction while it can be enhanced at moderate temperature by reducing the rate of the second reaction. This theoretical framework can be adopted to guide the development of highly selective catalyst for two-reactions-in-series systems, and it could be the basis for the development of assignment criteria of overall controlling factors for higher-number multiple reactions in series and reactions in parallel.

6 Author information

Corresponding author:

Musa Najimu: Department of Chemical and Environmental Engineering, University of California, Riverside, Riverside California 92507, United States Email: mnajimu@uci.edu, musan@ucr.edu

Present address:

University of California, Riverside

Authors:

Lateef Adewale Kareem: Department of Mechanical Engineering, West Virginia University, West Virginia, United States

Sagir Adamu: Department of Chemical Engineering, King Fahd University of Petroleum and Minerals, Dhahran, Saudi Arabia

Kandis Leslie Gilliard-AbdulAziz: Department of Chemical and Environmental Engineering, University of California, Riverside, Riverside California 92507, United States

The authors declare no competing financial interest.

7 Acknowledgement:

This research has received no funding. MN acknowledges Professor Reyad Shawabkeh for the useful lecture and term project on the concept of reaction-diffusion model development.

The MATLAB code used to conduct this study can be made available upon reasonable request.

8 References

(1) Vos, H. J.; Heederik, P. J.; Potters, J. J. M.; Luyben, K. C. A. M. Effectiveness Factor for Spherical Biofilm Catalysts. *Bioprocess Eng.* **1990**, *5*, 63–72.

(2) Khan, N. A.; Alshammari, F. S.; Romero, C. A. T.; Sulaiman, M.; Laouini, G. Mathematical Analysis of Reaction–Diffusion Equations Modeling the Michaelis–Menten Kinetics in a Micro-Disk Biosensor. *Molecules* **2021**, *26* (23), 7310.

(3) Thornburg, N. E.; Ness, R. M.; Crowley, M. F.; Bu, L.; Pecha, M. B.; Usseglio-Viretta, F. L. E.; Bharadwaj, V. S.; Li, Y.; Chen, X.; Sievers, D. A. Mass Transport Limitations and Kinetic Consequences of Corn Stover Deacetylation. *Front. Energy Res.* **2022**, *10*, 144.

(4) Zhang, L.; Zhang, H.; Ying, W.; Fang, D. Dehydration of Methanol to Dimethyl Ether over Γ-Al2O3 Catalyst: Intrinsic Kinetics and Effectiveness Factor. *Can. J. Chem. Eng.* **2013**, *91* (9), 1538–1546.

(5) Kim, D. H.; Lim, M. S. Kinetics of Selective CO Oxidation in Hydrogen-Rich Mixtures on Pt/Alumina Catalysts. *Appl. Catal. A Gen.* **2002**, *224* (1–2), 27–38.

(6) Lee, J. K.; Ko, J. B.; Kim, D. H. Methanol Steam Reforming over Cu/ZnO/Al2O3 Catalyst: Kinetics and Effectiveness Factor. *Appl. Catal. A Gen.* **2004**, *278* (1), 25–35.

(7) Al-Khattaf, S.; Atias, J. A.; Jarosch, K.; De Lasa, H. Diffusion and Catalytic Cracking of 1, 3, 5 Tri-Iso-Propyl-Benzene in FCC Catalysts. *Chem. Eng. Sci.* **2002**, *57* (22–23), 4909–4920.

(8) Konno, H.; Okamura, T.; Kawahara, T.; Nakasaka, Y.; Tago, T.; Masuda, T. Kinetics of N-Hexane Cracking over ZSM-5 Zeolites–Effect of Crystal Size on Effectiveness Factor and Catalyst Lifetime. *Chem. Eng. J.* **2012**, *207*, 490–496.

(9) Jones, R. E.; Gittleson, F. S.; Templeton, J. A.; Ward, D. K. A Simple Model for Interpreting the Reaction–Diffusion Characteristics of Li-Air Batteries. *J. Electrochem. Soc.* **2017**, *164* (1), A6422.

(10) Le, T. D.; Lasseux, D.; Nguyen, X. P.; Vignoles, G.; Mano, N.; Kuhn, A. Multi-Scale Modeling of Diffusion and Electrochemical Reactions in Porous Micro-Electrodes. *Chem. Eng. Sci.* **2017**, *173*, 153–167.

(11) Cutlip, M. B. An Approximate Model for Mass Transfer with Reaction Inporous Gas Diffusion Electrodes. *Electrochim. Acta* **1975**, *20* (10), 767–773.

(12) Wang, X.; Wang, B.; Meyerson, M.; Mullins, C. B.; Fu, Y.; Zhu, L.; Chen, L. A Phase-Field Model Integrating Reaction-Diffusion Kinetics and Elasto-Plastic Deformation with Application to Lithiated Selenium-Doped Germanium Electrodes. *Int. J. Mech. Sci.* **2018**, *144*, 158–171.

(13) Weisz, P. B. Diffusion and Chemical Transformation: An Interdisciplinary Excursion. *Science (80-.).* **1973**, *179* (4072), 433–440.

(14) Thiele, E. W. Relation between Catalytic Activity and Size of Particle. *Ind. Eng. Chem.*

1939, *31* (7), 916–920.

(15) Voge, H. H.; Morgan, C. Z. Effect of Catalyst Particle Size on Selectivity in Butene Dehydrogenation. *Ind. Eng. Chem. Process Des. Dev.* **1972**, *11* (3), 454–457.

(16) Zeldovich, Y. B. On the Theory of Reactions on Powders and Porous Substances. *Acta Physicochim. URSS* **1939**, *10*, 583.

(17) Weisz, P. B.; Prater, C. D. Interpretation of Measurements in Experimental Catalysis. In *Advances in catalysis*; Elsevier, 1954; Vol. 6, pp 143–196.

(18) Fogler, H. S.; Fogler, S. H. *Elements of Chemical Reaction Engineering*; Pearson Educacion, 1999.

(19) Chmelik, C.; Liebau, M.; Al-Naji, M.; Möllmer, J.; Enke, D.; Gläser, R.; Kärger, J. One-shot Measurement of Effectiveness Factors of Chemical Conversion in Porous Catalysts. *ChemCatChem* **2018**, *10* (24), 5553.

(20) Alopaeus, V. Approximating Catalyst Effectiveness Factors with Reaction Rate Profiles. *Catalysts* **2019**, *9* (3), 255.

(21) Dudukovic, M. P. Catalyst Effectiveness Factor and Contacting Efficiency in Trickle-Bed Reactors. *AIChE J.;(United States)* **1977**, *23* (6).

(22) Pagis, C.; Meunier, F.; Schuurman, Y.; Tuel, A.; Dodin, M.; Martinez-Franco, R.; Farrusseng, D. Demonstration of Improved Effectiveness Factor of Catalysts Based on Hollow Single Crystal Zeolites. *ChemCatChem* **2018**, *10* (20), 4525–4529.

(23) Roberts, G. W.; Satterfield, C. N. Effectiveness Factor for Porous Catalysts. Langmuir-Hinshelwood Kinetic Expressions. *Ind. Eng. Chem. Fundam.* **1965**, *4* (3), 288–293.

(24) Roberts, G. W.; Satterfield, C. N. Effectiveness Factor for Porous Catalysts. Langmuir-Hinshelwood Kinetic Expressions for Bimolecular Surface Reactions. *Ind. Eng. Chem. Fundam.* **1966**, *5* (3), 317–325.

(25) Lee, J.; Kim, D. H. An Improved Shooting Method for Computation of Effectiveness Factors in Porous Catalysts. *Chem. Eng. Sci.* **2005**, *60* (20), 5569–5573.

(26) Lattanzi, A. M.; Pecha, M. B.; Bharadwaj, V. S.; Ciesielski, P. N. Effect of Catalysts Particle Size on Selec. *Chem. Eng. J.* **2020**, *380*, 122507.

(27) Peters, B. Secondary Effectiveness Factors and Solubility Effects for Catalytic Reactions in Series. **2020**.

(28) Shayesteh Zadeh, A.; Peters, B. Secondary Effectiveness Factors for Catalytic Reactions in Series: Extension to Slab, Cylindrical, and Spherical Geometries. *React. Chem. Eng.* **2020**, *5* (10), 2003–2008.

(29) Bösenhofer, M.; Harasek, M. Non-Isothermal Effectiveness Factors in Thermo-Chemical Char Conversion. *Carbon Resour. Convers.* **2021**, *4*, 47–54.

(30) Carberry, J. J. The Catalytic Effectiveness Factor under Nonisothermal Conditions. *AIChE J.* **1961**, *7* (2), 350–351.

(31) Mingle, J. O.; Smith, J. M. Effectiveness Factors for Porous Catalysts. *AIChE J.* **1961**, *7* (2), 243–249.

(32) Kaczmarski, K.; Szukiewicz, M. K. An Efficient and Robust Method for Numerical Analysis of a Dead Zone in Catalyst Particle and Packed Bed Reactor. *Eng. Reports* **2021**, *3*, 12370.

(33) Maymo, J. A.; Cunningham, R. E.; Smith, J. M. Thermal Effectiveness Factors. *Ind. Eng. Chem. Fundam.* **1966**, *5* (2), 280–281.

(34) Tesser, R.; Di Serio, M.; Santacesaria, E. Catalytic Oxidation of Methanol to Formaldehyde: An Example of Kinetics with Transport Phenomena in a Packed-Bed Reactor. In *Catalysis Today*; Elsevier, 2003; Vol. 77, pp 325–333.

(35) Wheeler, A. Reaction Rates and Selectivity in Catalyst Pores. *Adv. Catal.* **1951**, *3* (C), 249–327. https://doi.org/10.1016/S0360-0564(08)60109-1.

(36) Santacesaria, E.; Morbidelli, M.; Carrà, S. Kinetics of the Catalytic Oxidation of Methanol to Formaldehyde. *Chem. Eng. Sci.* **1981**, *36* (5), 909–918. https://doi.org/10.1016/0009-2509(81)85045-2.

(37) Kolovertnov, G. D.; Boreskov, G. K.; Dzisko, V. A.; Popov, B. I.; Tarasova, D. V; Belugina, G. C. Study on Iron-Molybdenum Oxide Catalysts for the Oxidation of Methanol to Formaldehyde. I. Specific Activity as a Function of the Catalyst Composition. *Kinet. Catal.(Engl. Transl.)* **1965**, *6* (6), 950.

(38) Leroy, J.-M.; Peirs, S.; Tridot, G. Étude Physicochimique de Composés Ternaires Fe-Mo-O Pour Applications Catalytiques. *Comptes Rendus Acad. Sc. Paris, Ser. C* **1971**, *218*.

(39) Acosta, G.; Martinez, B.; Guzman, C.; De la Torre, I. *Kinetics and Preparation of Fe/Mo Catalysts for Methanol Oxidation to Formaldehyde*; 1979.

(40) Stiles, A. B.; Koch, T. A.; Dekker, M. Oxidation Catalysts: In Catalyst Manufacture. Marcel Dekker, New York 1995.

(41) Aruanno, J.; Wanke, S. Effect of High Temperature Treatment on the Properties of Fe-mo Oxide Catalysts. *Can. J. Chem. Eng.* **1975**, *53* (3), 301–307.

(42) Marcinkowski, M. D.; Yuk, S. F.; Doudin, N.; Smith, R. S.; Nguyen, M. T.; Kay, B. D.; Glezakou, V. A.; Rousseau, R.; Dohnálek, Z. Low-Temperature Oxidation of Methanol to Formaldehyde on a Model Single-Atom Catalyst: Pd Atoms on Fe3O4(001). *ACS Catal.* **2019**, 10977–10982.

(43) Trifiro, F.; Notarbartolo, S.; Pasquon, I. The Nature of the Active Component in a Fe2O3 MoO3 Catalyst: II. Study of the Variations Occurring during High Temperature Treatment. *J. Catal.* **1971**, *22* (3), 324–332.